Article | Received 30 October 2025; Revised 2 February 2026; Accepted 13 March 2026; Published 22 May 2026
https://doi.org/10.55092/esp20260002

Artificial Intelligence (AI)-enabled multimodal & cross spectrum photodetectors for management of diabetic foot ulcers

Ioannis Rallis[1,*], Aikaterini Angeli[2], Anastasios Doulamis[1] and Nikolaos Doulamis[1]

[1] Photogrammetry and Computer Vision Laboratory, School of Rural, Surveying and Geoinformatics Engineering, National Technical University of Athens, Athens, Greece
[2] Vascular Surgery Department, School of Medicine, National Kapodistrian University of Athens, Athens, Greece

* Correspondence author; E-mail: irallis@central.ntua.gr.

Highlights:

- Diabetic foot ulcer detection using computer vision tools and machine learning algorithms.
- A new photonics-based device for diagnosis and management of diabetic foot ulcers.
- Medical validation on a set of recruited patients for assessing diabetic foot ulcers.
- Experimental results on real-life patients of diabetic foot ulcers.

Abstract: Diabetes mellitus represents a major public health concern worldwide, with an estimated prevalence of approximately 9.1% of the population in Europe imposing a substantial economic burden on healthcare systems. One of the main complications of diabetes is the presence of Diabetic Foot Ulcers (DFUs) arising primarily from neuropathic and vascular impairments. Recent advances in sensing devices and photonics have stimulated the launch of sensors and imaging modules that can early diagnosis and prevent DFUs. In this paper we present the results of a new innovative, reliable, and cost-effective photonic-based system for the monitoring and management of DFUs, designed for large-scale clinical and home use. The system, developed within the framework of the H2020 PHOOTONICS project, integrates passive infrared photodetectors with active illuminators to achieve enhanced diagnostic capability. In PHOOTONICS project, two new photonic technologies for the early diagnosis and the management of diabetic foot have been developed; The professional device, called PRO and the home device called, HOME. The PRO version is dedicated for physicians at their offices or at hospitals. In this article, we present the clinical validation results of the new photonic-based device for diabetic foot ulcer. The results have been validated across four hospitals; ATTIKON University Hospital (Greece), VBMS University Hospital (Romania), CHARITE University Hospital (Germany), LEIDEN University Hospital (Netherlands). The validation includes (i) requirement process of diabetic and non-diabetic patients, patients stratification procedures, existence of comorbidities and an AI-based assessment of the results. For the latter we utilize ResNet deep models.

Keywords: diabetic foot ulcers; image segmentation; deep learning classification; photonics-based device; medical validation

1. Introduction

Diabetes mellitus represents a major public health concern in Europe, with an estimated prevalence of approximately 9.1% of the population. This condition imposes a substantial economic burden on healthcare systems, with direct annual costs estimated at €7–10 billion across the European Union [1]. The need for effective interventions to prevent and manage diabetes-related complications is therefore pressing. At the global level, the World Health Organization has documented a significant increase in the prevalence of diabetes among adults over 18 years of age, rising from 4.7% in 1980 to 8.5% in 2014. This corresponds to 422 million affected individuals worldwide, with current projections indicating a continued upward trajectory rather than a decline [2].

Diabetic foot ulcers (DFUs) represent one of the most prevalent and severe complications of diabetes, arising primarily from neuropathic and vascular impairments. Epidemiological evidence indicates that up to 4% of individuals with diabetes develop a foot ulcer annually, while 10%–15% are expected to experience at least one episode during their lifetime [3]. Chronic DFUs constitute a leading cause of hospitalization among diabetic patients and account for approximately 50% of all non-traumatic lower-limb amputations. The economic burden is considerable, as the cost of care for patients increases by a factor of 5.4 following the onset of the first ulcer, owing to higher rates of emergency department visits and prolonged hospitalizations. In parallel, the global market for diabetes diagnostic devices and systems, valued at $9.04 billion in 2014, is projected to reach $14 billion by 2022, reflecting both the scale of the clinical problem and the growing demand for effective monitoring technologies.

Recently, photonic sensing technologies have been explored heavily in medicine. One such example is Hyperspectral Imaging (HSI), also called imaging spectroscopy, originated from remote sensing, environmental and military applications, but it has been recently explored in many medicine applications [4]. HSI generates a three-dimensional (3D) hypercube that includes spatial and spectral information and covers a contiguous portion of the light spectrum up to few hundreds of bands able to identify pathological conditions in body tissues and offer potential for non-invasive disease diagnosis and surgical guidance in real-time. Light delivered to the biological tissue undergoes multiple scattering due to the inhomogeneity of biological structures and absorption primarily in hemoglobin, melanin, oxygen, elastin, collagen and water. It is assumed that the absorption, fluorescence, and scattering of a tissue change during the progression of a disease and/or under different functional conditions of an organ. Therefore, the reflected, fluorescent, and transmitted light from tissue captured by HSI carries quantitative diagnostic information about tissue pathology [5]. Light entering biological tissue undergoes multiple scattering and absorption events as it propagates across the tissue [6]. Biological tissues are heterogeneous in composition with spatial variations in optical properties [7]. The scattering properties of support tissues composed of cells and extracellular proteins (elastin, collagen, *etc.*) are caused by the small-scale inhomogeneities and the large-scale variations in the structures they form. The penetration depth of light into biological tissues depends on how strongly the tissue absorbs light. Most tissues are sufficiently weak absorbers to permit significant light penetration within the therapeutic window, ranging from 600 to 1300 nm. During absorption processing, transitions between two energy levels of a molecule that are well defined at specific wavelengths could serve as a spectral fingerprint of

the molecule for diagnostic purposes. For example, absorption spectra characterize the concentration and oxygen saturation of hemoglobin, metrics which are very important for vascular diseases.

Nowadays, medical research studies and clinical trials prove that HSI is an efficient sensing instrument for the assessment and prediction of diabetic foot ulceration and wound healing. The basic concept of the HSI system (operating at (700 nm–1300 nm) Near Infrared-NIR spectrum) utilizes the biomarkers of oxyhemoglobin (HbO_2) and deoxyhemoglobin (Hb), through which the Peripheral Oxygen Saturation (SpO_2) and Tissue Oxygen Saturation (StO_2) is computed, in the upper layers of skin on the foot as: a metric for assessing wound healing, a reflection of microvascular disease, and determining tissue at risk for forming new ulcers. More specifically, the Cleveland Clinic in USA in collaboration with UCLA and University of Pennsylvania has performed a clinical trial of hyperspectral imaging to access and predict DFUs. This study compared a cohort of 210 high risk diabetic subjects (90 of Type 1 and 120 of Type 3) over a period of 18–24 months. The study took place at three medical centers, each enrolled 70 subjects [8]. The results indicate that HSI is an efficient tool for DFU prediction as well as healing study. Similarly, the research in [9] proves that medical HIS technology is adequate to evaluate micro-circulation changes in a diabetic foot ulcer.

To address the aforementioned difficulties, in [10] we have developed an innovative, reliable, and cost-effective photonic-based system for the monitoring and management of DFUs, designed for large-scale clinical and home use. The system, developed within the framework of the H2020 PHOOTONICS project, integrates passive infrared photodetectors with active illuminators to achieve enhanced diagnostic capability [11]. Specifically, the proposed platform incorporates: (i) a passive hyperspectral imaging (HSI) photodetector sensitive to the near-infrared (NIR) spectrum (700–1000 nm), combined with a tunable diode illuminator operating within the same spectral range, in order to optimize sensitivity, specificity, and accuracy in detecting peripheral oxygenation and tissue saturation (SpO_2/StO_2), as well as oxyhemoglobin/deoxyhemoglobin ratios, at a spatial resolution of approximately 50 pixels/cm; (ii) a passive mid-infrared (Mid-IR) photodetector (5.7–9.3 μm) coupled with a Quantum Cascade Laser (QCL), designed to capture additional biochemical and structural tissue attributes, including elastin, collagen, lipids, amino acids, and carbohydrates, which are critical for early DFU prediction and clinical management, at a resolution of ~10 pixels/cm; and (iii) a thermal-infrared sensing module capable of detecting localized hyperthermic and hypothermic distributions within regions of interest, with resolution specifications tailored to the professional (full HD) and simplified in-home (10 pixels/cm) device configurations. The system requirements of this device are also presented in [11].

In PHOOTONICS project, two new photonic technologies for the early diagnosis and the management of diabetic foot have been developed; The professional device, called PRO and the home device called, HOME. The PRO version is dedicated for physicians at their offices or at hospitals. It enhances the In-Home version by including the (i) optimized HSI sensor, combining with the IR hyperthermia photodetector, (ii) the optimized Mid-IR Sensor and (iii) the activities HSI illuminator to increase reliability and provide measurements of additional attributes (e.g. tissue properties), while simultaneously keeping the cost affordable for professional use. The In-Home version is designed to be dedicated for patients. It includes the optimized low-cost IR sensor with the embedded signal/processing tools in order to increase the resolution performance, reduce noise and provides high-level decision-making mechanism.

The system is equipped with advanced AI algorithms as described in Section 6. More specifically, a Convolutional Neural Networks (CNN) architecture has been developed for detecting the diabetic foot ulcers. A ResNet architecture is adopted as an efficient implementation of the CNN [12]. The role of this model is to extract automatically salient features from the images. Deep learning models like U-net are also used for segmenting the wound regions and automatically detect Regions of Interest (ROIs). The models take into account different variations in lighting and visual conditions [13,14].

In this article, we present the clinical validation results of the new photonic-based device for diabetic foot ulcer. The results have been validated across four hospitals; ATTIKON University Hospital (Greece), VBMS University Hospital (Romania), CHARITE University Hospital (Germany), LEIDEN University Hospital (Netherlands). The validation includes (i) requirement process of diabetic and non-diabetic patients, patients stratification procedures, existence of comorbidities and an AI-based assessment of the results.

Initially, we describe shortly some relevant papers in Section 2. Then, the main steps for the medical valdiation executed in ATTIKON hospital have been discussed in Section 3. This includes the preparation of the medical validation, the patients' recruitment procedures and the installation of the HOME and PRO devices. Section 4 shows the results of the medical validation while Section 5 presents the medical validation. The AI-based analysis of the results is shown in Section 6 and in Section 7 we show a statistical analysis. Finally Section 8 presents the AI-driven feature extraction models and Section 9 concludes the paper.

2. State-of-the-art description

2.1. Current clinical practice and its limitations

Standard DFU risk assessment relies on a combination of manual clinical tests: (i) Neuropathy Assessment: The Semmes-Weinstein (SW) 10-gram monofilament test detects loss of protective sensation with sensitivity 80%–90% for identifying neuropathy. However, neuropathy alone does not reliably predict ulcer formation; ~60%–70% of patients destined for DFU present with abnormal SW testing, but many diabetics with abnormal sensation never develop ulcers [15]. (ii) Vascular Assessment: The Ankle-Brachial Index (ABI) measures systolic blood pressure at the ankle *vs.* brachial artery, yielding a single ratio (normal > 0.9, borderline 0.71–0.9, severe peripheral arterial disease < 0.7). ABI sensitivity for detecting proximal arterial stenosis is ~75%–80%, but this measurement provides no information about microvascular perfusion distribution across the foot, tissue-level oxygen saturation (SpO_2/StO_2), capillary bed reactivity and temporal changes or trends [16].

2.2. Advanced optical imaging for DFU

RGB Imaging with Deep Learning: Studies from 2020–2024 report CNN classification of foot photographs achieving 85%–92% accuracy for ulcer/no-ulcer discrimination [17,18]. Advantages include simple deployment (smartphone-based systems under development) and established datasets (DFUC 2020, DFU_Seg public databases). Limitations include dependence on lighting conditions, inability to assess vascular/metabolic parameters beyond visual appearance, and single-site validation bias.

Thermal Imaging: The Cleveland Clinic conducted a prospective trial (n = 210 high-risk patients, 18–24 month follow-up) demonstrating that thermal asymmetry (temperature difference between feet > 2 ℃) is a significant predictor of subsequent ulcer development [19]. Our work extends this literature by automating thermal analysis via ResNet-18 deep learning, replacing subjective manual temperature assessment with quantitative algorithmic classification.

Hyperspectral Imaging: NIR hyperspectral imaging (700–1000 nm) can non-invasively estimate tissue oxygen saturation (SpO_2, StO_2) by quantifying oxyhemoglobin and deoxyhemoglobin concentrations via spectral unmixing [19]. Mid-infrared (mid-IR) spectroscopy (5.5–12.4 μm) reveals biochemical signatures of tissue composition: elastin and collagen cross-linking patterns, glucose concentration, water content, and lipid profiles. These biomarkers precede clinical symptoms by 7–14 days, offering potential for early warning [20]. However, clinical deployment of hyperspectral imaging remains largely research-phase; no integrated multi-modal device combining thermal, NIR, and mid-IR had been deployed in clinical settings prior to PHOOTONICS.

Wearable Sensors: Plantar pressure insoles (e.g., Tekscan InSole, Delft University systems) provide continuous monitoring of pressure distribution, enabling prediction of ulcer risk with ~75%–80% accuracy [21]. Advantages include continuous monitoring and home deployment. Limitations include reliance on pressure data alone (insufficient without vascular/biochemical assessment) and requirement for continuous device wear. Color Doppler ultrasound (CDU) offers superior anatomical detail (sensitivity/specificity 85%–95%) but is operator-dependent, time-consuming (20–30 min per patient), and available primarily at tertiary centers.

Some other works have been proposed in the literature for diabetic foot ulcers using computer vision and Artificial Intelligence (AI) techniques. Some first results on the use of image analysis techniques have been proposed in [22]. In [23] several computer vision algorithms are proposed for detecting ulcers in feet. Unsupervised clustering techniques for grouping the type of ulcers under an automatic way has been proposed in [24]. In [25] these novel AI-driven and computer vision tools have been embedded in a complete intelligent care management system. Another work that exploits Internet of Things (IoT) concepts for detecting foot ulcers has been presented in [26]. The work of [27] has extended the previous outcomes by focusing more on real-time analysis and the utilization of parallel hardware computational tools.

A systematic review of different algorithms has been proposed in [28]. In this paper, the authors present the challenges on machine learning algorithms and computer vision-based classification tools to analyse the diabetic foot ulcer images.

2.3. System specifications

The details of the specifications of our systems have been presented in [11]. However, for clarity of presentation we summarize in this subsection the main specifications elements. Our system consists of an RGB optical sensors, a thermal sensor, a hyperspectral image and a pressure sensor. A very cheap led-based RGB sensor is employed in our device of white light source. The size of the sensor is tiny so as to be easily embedded in the HOME edition of our device. For the thermal sensor, we use the commercial product of FLIR thermal cameras. In particular, two different types of cameras have been selected. The first is the FLIR T1030SC camera of high sensitivity adopted for the PRO edition while the second is the FLIR ONE PRO thermal camera chosen for the in-home edition. The hyperspectral

sensor used for our device has been manufactured by IMEC R&D hub for nano- and digital technologies in Belgium. The sensor is based on Fabry–Pérot structures. Regarding the pressure sensor, our device uses the pressure mapping sensor from Tekscan. This sensor is based on tactile array sensors (ultra-thin pressure-sensitive resistors). In the professional edition, a mid-infrared sensor has been also added. More specifically, we use broadly tuneable mid-infrared external cavity quantum cascade lasers (ECQCLs) to perform laser direct infrared spectroscopy of the patient's feet.

3. The steps of the medical validation

3.1. Preparation of the medical validation

For the preparation of the medical validation, all the activities introduced in the previous months were intensified. Initially, the four hospitals' lists of candidates for the recruitment were updated. Medical researchers contacted their colleagues of diabetes-related departments (internal medicine, endocrinology, neurology, surgery), aiming to disseminate the purposes and the objectives of PHOOTONICS project, and attempting to attract new candidates. Candidates approached in the previous period, being already in the waiting list, but having in the meanwhile lost their eligibility criteria, or wishing to redraw their consent to participate in PHOOTONICS study were excluded, while were replaced by new ones, provided by the registries of Hospitals' Department of Outpatient Diabetic Foot Management. Active participants contact details were kept in each pilot's internal department database where no access was possible to third parties for accordance to GDPR issues.

3.2. Recruitment procedures

In this medical validation there are three groups (with a possible fourth group): 1st group: diabetic patients without a DFU (patients with a previous DFU that is healed by the time of recruitment, are also considered eligible for this group). 2nd group: diabetic patients with an active DFU (ranging from minor to major). 3rd group: non-diabetic patients without a foot ulcer (control group).

During the period of the medical validation of the PHOOTONICS project [11], the ATTIKON university hospital underwent the following recruitment procedure. A number of twenty-five (25) participants were enrolled in the study at Attikon University Hospital. Participants entering the study were provided the protocol synopsis at least 24hours before recruitment, to reassure their informed consent.

3.3. Installation of the PHOOTONICS device

3.3.1. Home device

Storage of the packing box: The HOME device packing box was a large wooden box, which was stored in a safe, dry place in the Hospital. This box may be used for packaging in case of a future device transportation. Installation of the device: The HOME device was placed in a room not exposed to extreme sunlight, where temperature and humidity range are within a narrow range. In this room, temperature-regulating systems are in use (air conditioner, central heat system) reaching a steady room temperature of about 24 ℃. In addition, sterilizers are available in place and a secure WIFI connection is reassured.

Training of the medical staff: With the technical assistance of the project partners, the medical personnel engaged to the study have been trained in the use of the device. Three training sessions were required in ATTIKON University Hospital for the medical doctors to acquire the skills for the device use. Four researchers have been trained in using the HOME device in the Greek pilot.

3.3.2. Professional device

During the installation of the PRO PHOOTONICS device in the ATTIKON university hospital, the device has been tested and calibrated for a real-life operational setting. In this sub-section, we discuss some issues regarding the user interface and the operational settings of the PRO device. Figure 1 presents a shot of HOME PHOOTONICS device. Figure 2 presents the final installed PRO device in ATTIKON Hospital.

Figure 1. The HOME demonstrator device, including the photonic technologies, server and image processing center.

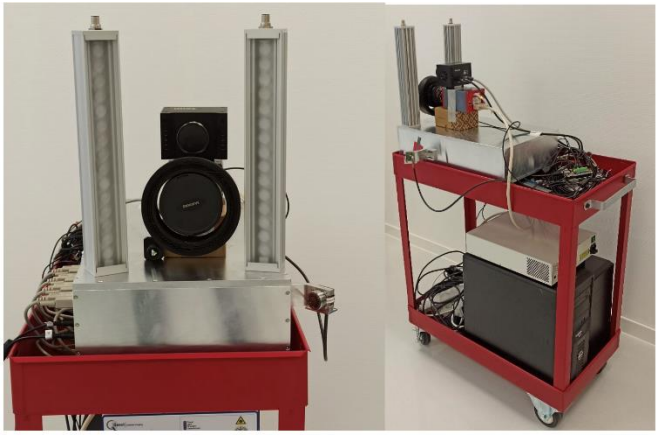

Figure 2. The PRO demonstrator device, including the photonic technologies, server and image processing center.

4. Results regarding the medical validation

Measurements with the PHOOTONICS device has been a subject of validation, as follows:

Time required for the HOME device measurements: The time required for one individual and both leg measurements was proved to be short, on average 10 min. However, this time refers only to the PHOOTONICS sensors calibration and measurements. If clinical and laboratory data were additionally

to be entered, the respective time increased to about 20 min. Finally, if clinical examination has to take place in the same session, the time required for one person is approximately 45 min. For this reason, it was advised that clinical examination, and the entering of clinical and laboratory data to the device should take place separately from the measurements.

Flexibility of the procedure: The procedure of HOME device measurements has been considered flexible, as:

- Fields can be skipped and going to the next app page is allowed.
- The participant's file can be edited and updated any time.
- The device can be easily transferred to another place if required.

Participant convenience: Measurements by the HOME device were convenient for the participants, as:

- They experienced no pain throughout the procedure.
- The time required for the measurements was short. However, few limitations were noticed towards participant convenience, such as:
- Measurements were conducted far from the yard. In the second phase of measurements by the dedicated sensor for each leg, participants were supposed to place the limb closer to the light source. This leg position was slightly uncomfortable for most of the participants.

Self-measurements applicability: The HOME device was initially planned to be also used by the diabetic patients themselves, in order to assess the ease-of-use of the device. An assessment questionnaire was designed as feedback on the use of the PHOOTONICS HOME device during the validation. It is meant to record and assess the usability and effectiveness of the device, particularly from the perspective of patients who may include healthy individuals as well as diabetic patients with or without a DFU. This questionnaire, which is specifically designed to be filled in by the clinical staff responsible for the measurements, records the patient's experience and identifies any challenges they may have faced. The ultimate goal is to make necessary improvements to enhance the device's user-friendliness and overall performance. At this stage of the study however, the large volume of the device and the need to make actions on the front screen, while having the leg of interest in the back side, render the self-measurements very difficult and of no major benefit to the patient and the study itself. This will be considered as an option at the second phase of the medical validation.

5. Medical validation results

Data from the sensors and clinical data were analysed and any possible correlations were investigated by traditional statistical tests and AI algorithms. All data were formulated to join either categorical, ordinal or numerical classes and to expedite the statistical analysis. The table below summarizes the clinical assessment outcomes. Table 1 shows a synopsis of the clinical validation results. The main steps are: (a) the clinical infrastructure including clinical validation preparations for the clinical study, (b) the patients' recruitment procedures, (c) the archiving of the medical information, (d) data anonymization and assessment, (e) the execution of the laboratory tests, and (f) the assessment of the new device.

Table 1. A synopsis of the clinical validation results in the ATTIKON University Hospital.

Clinical assessment elements	Short description	Targets of the clinical assessment	Achievements of the targets
Clinical infrastructure	Validation of the preparation for the clinical studies (e.g., rooms, personnel, wifi and communication connections).	Dedicated room, fulfilling clinical examination specifications.	One clinical examination room. One backup reservation room.
Recruitment procedures	Evaluation of the recruitment items required for PHOOTONICS clinical study (GDPR documents, consent forms).	Documents for recruitment. Personnel assisting recruitment. Lists of candidates (registries of Outpatient Diabetic Foot Department). Time scheduling for the recruitment appointments.	Recruitment documents readily available in dedicated boxes in the Hospital. Review and update of the lists of candidates by dedicated staff. Calendar for Allocation of appointments.
Medical information info archiving	Assessment of the patients' medical history record archived by recruitment procedure.	Filling the fields of the medical history. Verifying inclusion/exclusion criteria. Collecting data on personal habits (smoking, alcohol consumption, diet). Archiving diabetes type, severity, treatment, complications and comorbidities.	All fields of medical history templates are filled. Inclusion/exclusion assessment has been performed by medical experts. Complimentary information has been collected upon medical experts' request.
Data assessment	Verify the data pseudoanonymization procedure adopted throughout the recruitment process.	Participants personal and clinical data are handled in the based on the institution's internal regulation and the PHOOTONICS legal documents.	All personal information and clinical data are pseudoanonymized with respect to GDPR principles.
Clinical and laboratory examination assessment	Evaluation of the clinical and laboratory (blood and functional) tests conducted to the recruited participants.	Participants are submitted standard and vascular clinical examination (thorax auscultation, peripheral pulses palpation, Ankle Brachial Index measurement…).	All of the recruited participants were clinically assessed and submitted to doppler measurements.
HOME device assessment—size/portability	Assessment of the storage capability and transportability of the device.	The size of the device is similar to the one of an ultrasound machine. The device is easily transportable by its steering wheels.	The HOME device's storage capability is of medium convenience. The HOME device's transportability is a feature supporting user friendliness.
HOME device assessment-feasibility	Evaluation of the feasibility of measurements with the HOME device by the medical experts.	Medical experts were trained to use the HOME device in two training sessions, assisted by technical partners.	Users interface was friendly for the medical investigators upon short time training sessions. Skipping steps and ability for editing was applicable for the medical investigators.
Home device assessment—pre-measurement procedure	Evaluation of the procedure before the actual measurements.	Evaluation of the procedure in terms of time and complexity.	Preparation for measurements required some time (starting the application, entering the participants' clinical data, calibrating for black and white).
HOME device assessment—applicability	Assessment of the convenience of measurements for the participants.	Measurements were assessed in terms of duration, pain experience and discomfort for the participants.	Measurements by HOME device were achieved in short times (about 10min) and with no experienced pain. In the first phase of measurement no discomfort was experienced by the participants. In the second phase of measurement minor discomfort was experienced because of the more extreme leg position.
HOME device assessment—operational accuracy	Evaluation of the ability of HOME device to undertake measurements which are anonymized, repeatable, editable and reliably stored.	Measurement by the HOME device is appropriately carried out.	For every new participant a personal ID is produced, not allowing for individual's recognition. The participants' file is accurately stored and be edited in a later phase and new data (clinical, laboratory *etc*.) can be entered.

For facilitating the reporting of historical, clinical and laboratory data in all pilots, a dedicated clinical data template was created. In this template, data mentioned are included. In addition, in this template, the historical, medical, clinical and laboratory data are transformed to values or classes that can easily be measured, reported, and compared to sensor data, to produce results towards any possible statistical correlations. Fields included in the PHOOTONICS clinical data template are depicted in Table 2. This table describes the data used and the possible values for these data. The categories are (a) demographic

and historic data, (b) personal data, (c) historic data for diabetes complications, (d) clinical data and (e) neurological examination. For each category, we describe both the data collected and the values of them.

Table 2. A synopsis of the common data template model used for clinical annotation of the collected data.

Data used for Clinical Annotation	Possible values	Data used for Clinical Annotation	Possible values
Demographic/Historical Data		**Personal Habits**	
Age	Years	Alcohol Consumption	No or Social drinking or Alcoholism
Gender	Male/Female	Smoking	Former < 10years
Weight	Kg	Exercise	No/Light/Intense
Height	cm	Diet	No/Diabetic/Full
Diabetes Treatment	Oral or Insulin or Both		
Malignancies	Yes/No	**History of Diabetes Complications**	
Previous Interventions	Surgery or Bypass or Angioplasty or Other	Eye	Yes/No
Diabetes Complications	Ulcer or Eye or Wound or Other	History of Right DFU	Yes/No
Smoking	Yes/No	History of Left DFU	Yes/No
Smoking Duration	Pack Years	Right Minor Amputation (digit, transmtetarsal)	Yes/No
Neurological Status	Stroke or TIA or Demyelinate Disorder or Other	Left Minor Amputation (digit, transmtetarsal)	Yes/No
Cardiovascular Status	AMI or Angina or Arrythmias or Heart Failure or Other	Right Major Amputation (below knee/above knee)	Yes/No
Vascular Status	PAD or Venous insufficiency or Vasculitis or Aneurysm or Other	Left Major Amputation (below knee/above knee)	Yes/No
Respiratory Status	Asthma or COPD or Other	Right Rest Pain	Yes/No
Digestive Status	Gastric ulcer or Colitis or Other	Left Rest Pain	Yes/No
Connective Tissue Diseases	Lupus Eryth or Reuh arthritis or scleroderma, Other	Right PAD with revascularization	Yes/No
Muscular and Bone Diseases	Yes/No	Left PAD with revascularization	Yes/No
Visual Disturbances	Glaucoma or Blindness or Other	Right Osteomyelitis	Yes/No
Prosthetic Materials	Yes/No	Left Osteomyelitis	Yes/No
Drug Regimens	Yes/No	Renal Failure	No or Yes Conservative or Yes Dialysis
Clinical Data		**Neurological Examinations**	
Right/Left neuropathic symptoms	Yes/No	Right/Left 1st Toe Plantar	Yes/No
Right/Left claudication	Yes/No	Right/Left 3rd Toe Plantar	Yes/No
Right/Left current DFU	Yes/No	Right/Left 5th Toe Plantar	Yes/No
Right Muscle Atrophy	Yes/No	Right/Left 1st Metatarsal Toe Plantar	Yes/No
Right/Left Toe Clawing	Yes/No	Right/Left 3rd Metatarsal Toe Plantar	Yes/No
Right/Left metatarsal head prominence	Yes/No	Right/Left 5th Metatarsal Toe Plantar	Yes/No
Right/Left Charcot Deformity	Yes/No	Right/Left	Yes/No
Right/Left Hyperceratosis	No or Diffuse or Heel or Localized on Plantar Area or Multiple	Right/Left Dorsal Surface	Yes/No
Right/Left onychomycosis	Yes/No		
Right/Left Tinea Pedis	Yes/No		
Right/Left Infection/Osteomyelitis Clinical or Radiological	Yes/No		

6. AI-based analysis of the results

Imaging toolkits play a pivotal role in the diagnosis, monitoring, and management of DFUs. Diabetic foot ulcers are a common and serious complication of diabetes, often leading to infection, hospitalization, and even amputation if not properly managed. Advanced imaging techniques, combined with machine learning models, particularly those based on CNNs, have become essential tools in the medical field for accurately detecting and characterizing these ulcers. The integration of imaging toolkits helps in various tasks such as feature extraction, prediction, segmentation, and semantic segmentation, which are crucial for effective wound assessment and treatment planning.

6.1. Feature extraction models for ulcer analysis

Feature extraction is a critical step in the analysis of diabetic foot ulcers, where specific characteristics of the wound, such as size, shape, depth, and texture, are identified from medical images. Traditional feature extraction methods might involve manual annotation and measurement by medical professionals, which can be time-consuming and prone to variability. However, modern imaging toolkits use automated feature extraction models that leverage deep learning algorithms to provide consistent and accurate analysis.

CNN-based models are particularly effective for this task. Pre-trained models, such as VGGNet, ResNet, and EfficientNet, can be adapted to extract relevant features from images of diabetic foot ulcers captured using modalities like digital photography, thermography, and hyperspectral imaging. These models can automatically learn discriminative features that are crucial for differentiating between various types and severities of ulcers, thereby assisting clinicians in diagnosing and grading the wounds. Figure 3 presents the adopted ResNet architecture for feature extraction.

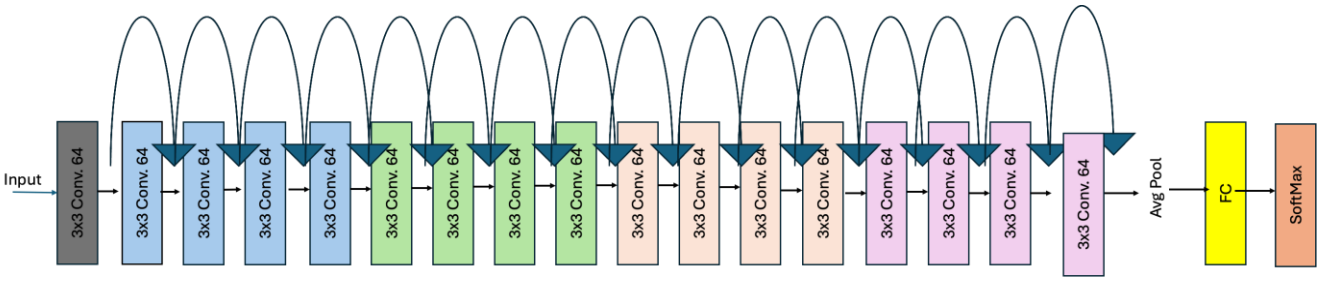

Figure 3. The adopted ResNet architecture for feature extraction.

This model is designed to analyze thermal images of diabetic foot ulcers to help identify important features that can aid in diagnosis and treatment planning. It starts by taking grayscale thermal images, which are pictures that show temperature variations, and prepares them for analysis. The model uses a pre-trained neural network called ResNet-18, which has been specially modified to work with these single-channel thermal images. By adjusting the first layer of the network, it can process the grayscale input instead of the usual color images. As the thermal images pass through the network, the model extracts important patterns and details that are difficult to see with the naked eye, like subtle temperature differences that might indicate areas of concern. This process results in a set of features for each image that can help doctors better understand the condition of a wound and make more informed decisions about patient care.

6.2. Convolutional neural networks for ulcer prediction

CNNs are widely used for the prediction of diabetic foot ulcer outcomes, such as the likelihood of healing or progression to more severe stages. These models are trained on large datasets of labelled images to recognize patterns associated with different ulcer characteristics. For example, CNNs can be used to predict whether an ulcer will heal with standard care or if it requires more aggressive treatment or surgical intervention.

Popular CNN architectures like InceptionNet and DenseNet are employed for their ability to learn complex feature hierarchies from ulcer images. These models can incorporate not only the visual data from the ulcer but also contextual information, such as surrounding tissue condition and signs of infection. By integrating multimodal data inputs, CNNs provide a more comprehensive assessment, enhancing the accuracy of ulcer outcome predictions and supporting evidence-based decision-making in clinical settings. It also handles differentiations in lighting and visual conditions

6.3. Segmentation models for wound delineation

Accurate segmentation of diabetic foot ulcers is essential for proper wound assessment and treatment planning. Segmentation involves delineating the ulcer area from surrounding healthy tissue in medical images, which is crucial for calculating the wound size, monitoring its progression, and guiding interventions. Manual segmentation is often challenging and subjective, but segmentation models provide an automated solution that enhances consistency and precision.

Deep learning-based models like U-Net, SegNet, and Mask R-CNN are specifically designed for medical image segmentation tasks. These models can accurately identify the boundaries of ulcers, differentiate between various tissue types, and assess the extent of necrosis or granulation tissue within the wound. Advanced segmentation models also enable 3D reconstruction of the wound, providing a more detailed analysis that can help in planning surgical procedures or other complex treatments.

6.4. Semantic segmentation for detailed wound analysis

Semantic segmentation takes the segmentation process a step further by classifying each pixel in an image into predefined categories such as ulcer, necrotic tissue, granulation tissue, and healthy skin. This pixel-level classification is particularly useful in diabetic foot ulcer management as it provides a detailed map of the wound area, allowing for precise monitoring of healing progress and identification of any complications such as infection or ischemia.

Models like DeepLab, PSPNet, and Fully Convolutional Networks (FCNs) are widely used for semantic segmentation tasks. These models can handle the variability in ulcer appearance due to factors such as lighting conditions, patient skin tone, and ulcer depth. By providing a detailed, pixel-wise understanding of the wound, semantic segmentation models assist clinicians in making more informed decisions regarding the type of treatment required, the frequency of dressing changes, and the need for surgical debridement or other interventions.

6.5. Multi-modal data fusion

Thermal, optical, and hyperspectral data can be combined for diabetic foot ulcer detection using multimodal data fusion, where information from each modality contributes complementary insights. After preprocessing and spatially aligning the images, features such as temperature patterns from thermal imaging, color and texture information from optical images, and spectral or physiological indicators from hyperspectral data are extracted. These features are then integrated—most commonly at the feature level—by concatenating and normalizing them into a unified representation that is input to a machine-learning or deep-learning model. This combined approach enhances robustness and diagnostic accuracy by jointly capturing inflammatory, visual, and physiological tissue changes.

7. Statistical analysis and clinical assessment

7.1. Presence of ulcer: diabetic foot ulcer classification

For the statistical analysis, all the participants were tested on the PHOOTONICS device and the intensity of the pixel created by the obtained thermal images were measured. The following table presents some indicative results of the pixel intensity data from thermal images of DFUs categorized into three groups: “DF with active ulcer,” “DF with healed ulcer,” and “DF without active/healed ulcer.” The pixel intensity metrics include mean, median, standard deviation (Sd), minimum (Min), and maximum (Max) thermal values for both the left and right foot of various patients. Table 1 (and the rest tables) indicates indicative patients ID for presentation purposes. Table 3 shows the statistical analysis results and the clinical assessment for the PHOOTONICS device. For patients with active ulcers, the mean pixel intensity values range from 29,826.08 to 30,466.64, indicating higher thermal readings, potentially due to inflammation or infection. The standard deviation (Sd) values for this group are also relatively high, suggesting significant variability in thermal intensities within the ulcerated regions. For patients with healed ulcers, the mean thermal values are slightly lower and less variable, ranging from 30,001.56 to 30,434.64, with corresponding median values closely aligned with the means, indicating a more uniform thermal distribution. The group without active or healed ulcers displays mean thermal values ranging from 29,873.54 to 29,987.68, which are generally lower and show higher standard deviations than the healed ulcer group, possibly reflecting normal thermal patterns in non-ulcerated feet. Overall, these results suggest that active ulcers exhibit higher and more variable pixel intensity values, while healed ulcers and non-ulcerated feet demonstrate lower, more stable thermal characteristics, which can be critical for distinguishing between different stages of diabetic foot conditions.

In Figure 4, we present the distribution of the feature for Diabetic Foot patients of an active ulcer, a healed ulcer and without an ulcer. These histograms illustrate the distribution of pixel intensities (in terms of the respective wavelength that these pixels correspond to) from thermal images of diabetic feet, categorized into three groups: feet with active ulcers, feet with healed ulcers, and feet without ulcers. The histograms in Figure 4a show the pixel intensity distributions for diabetic feet with active ulcers, with noticeable peaks suggesting higher thermal activity or inflammation areas. Figure 4b represents feet with healed ulcers, where the histograms generally show a different pattern with peaks

at different intensities, reflecting changes in thermal characteristics due to healing processes. Lastly, Figure 4c displays the histograms for diabetic feet without any ulcers, where the pixel intensity distributions appear more uniform, indicating a lack of localized thermal anomalies typically associated with ulcers. These histograms are crucial for understanding the thermal patterns related to diabetic foot ulcers' presence, healing, and absence, providing insights for medical diagnosis and monitoring. For all histograms there is peak in all temperatures due to the cold background which also in included in these metrics. The background is common in all images, therefore all differences came from the feet measured.

Table 3. Statistical analysis and clinical assessment of the PHOOTONICS devices (The diabetic foot ulcer classification supercluster).

Presence of ulcer	**Patient ID**	**Left/Right Foot**	**Thermal Values**				
DF with active ulcer			**Mean**	**Median**	**Sd**	**Min**	**Max**
	20	left	30,037.77	29,968	192.47	29,764	30,947
	33	right	30,466.64	30,417	144.62	30,215	31,282
	14	right	29,826.08	29,707	313.34	29,401	30,626
	28	right	29,987.27	29,943	175.49	29,690	30,941
	28	left	30,315.35	30,244	210.81	30,008	31,441
DF with healed ulcer							
	33	left	30,434.64	30,371	157.64	30,199	31,192
	30	right	30,420.97	30,367	193.83	30,070	31,605
	27	left	30,081.56	29,983	319.93	29,624	31,365
DF without active/healed ulcer							
	21	right	29,873.54	29,737	322.39	29,497	30,675
	21	left	29,932.11	29,773	367.13	29,545	30,760
	22	right	29,987.68	29,860	330.49	29,460	30,842
	22	left	29,951.94	29,820	334.34	29,543	30,828

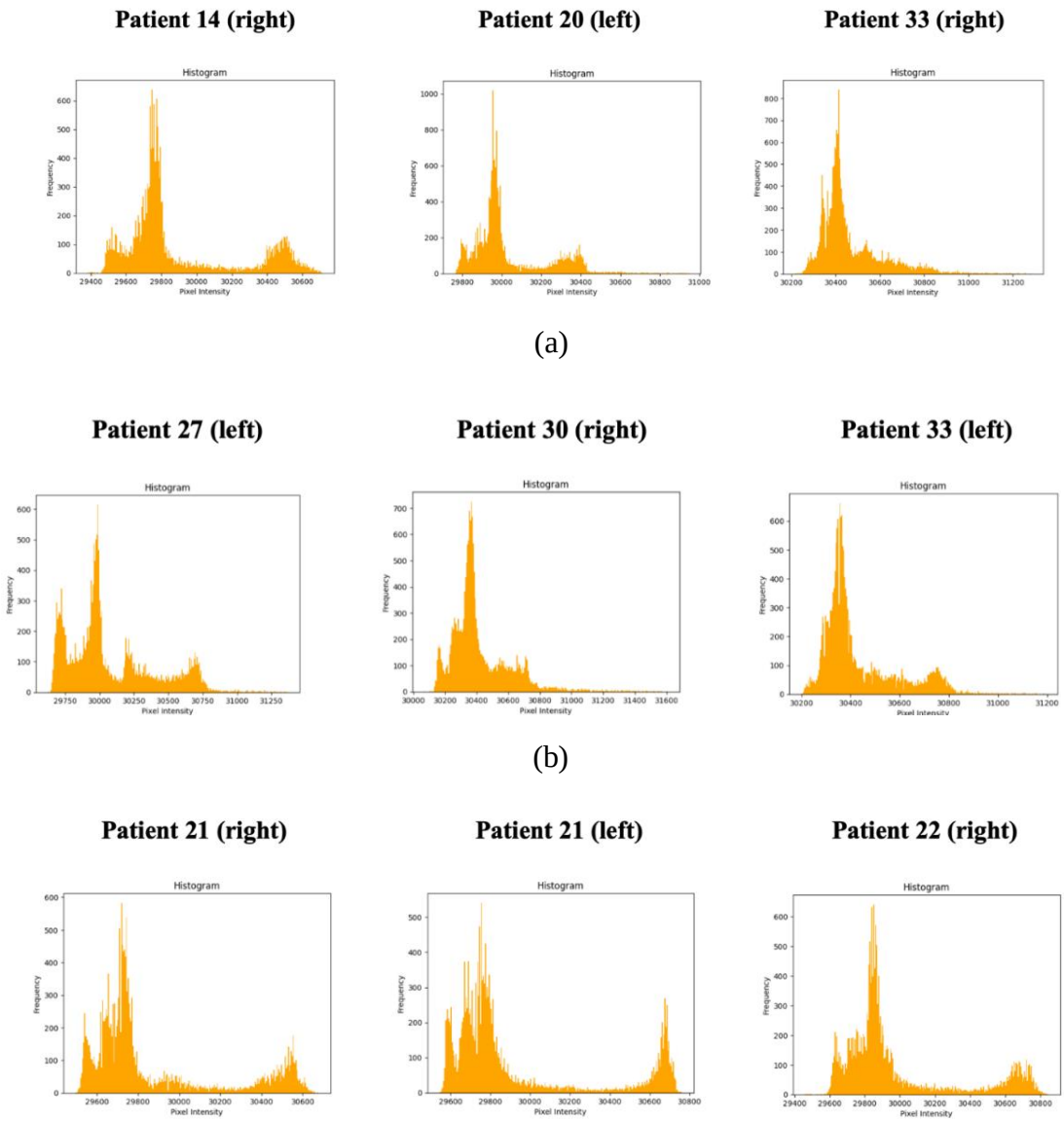

Figure 4. PHOOTONICS features for the DF with **(a)** active ulcer; **(b)** healed ulcer; **(c)** without an active ulcer. Pixel intensity is measured as the occurrence of the wavelengths.

7.2. Traditional tests for DF: the Semmes Weinstein approach

Table 4 presents descriptive statistics of pixel intensity from thermal images for diabetic foot (DF) ulcer evaluation, comparing patients with positive (abnormal) and negative (normal) results from Semmes Weinstein tests. The data, again, is split by patient ID and foot (left or right), with the thermal values reported in terms of mean, median, standard deviation (Sd), minimum (Min), and maximum (Max) pixel intensities. For patients with abnormal Semmes Weinstein results, the mean pixel intensity ranges from 29,886.95 to 30,315.35, with varying degrees of spread as indicated by the standard deviations. These values suggest higher variability in thermal readings for patients with impaired sensory function of the foot, reflecting the presence of abnormalities such as inflammation or infection.

Table 4. Statistical analysis of traditional tests for DF (The Semmes Weinstein tests—clinical assessment of a touch).

Traditional tests for DF	Patient ID	Left/Right Foot	Thermal Values				
Semmes Weinstein positive (abnormal)			**Mean**	**Median**	**Sd**	**Min**	**Max**
	28	right	29,987.27	29,943	175.49	29,690	30,941
	28	left	30,315.35	30,244	210.81	30,008	31,441
	27	left	30,081.56	29,983	319.93	29,624	31,365
	26	left	29,864	29,773	271.35	29,403	31,062
	20	right	29,987.27	29,943	175.49	29,690	30,941
	20	left	30,037.77	29,968	192.47	29,764	30,947
	14	right	29,896.95	29,769	323.74	29,381	30,712
	14	left	29,826.08	29,707	313.34	29,401	30,626
	12	right	29,979.38	29,948	216.6	29,621	31,302
	12	left	29,956.06	29,923	199.23	29,521	31,242
Semmes Weinstein negative (normal)							
	35	right	30,621.73	30,544	206.58	30,211	31,744
	35	left	30,605.27	30,538	208.21	30,288	31,744
	32	right	30,642.08	30,569	198.25	30,168	31,693
	32	left	30,592.4	30,510	199.11	30,302	31,636
	31	right	30,586.31	30,481	250.86	30,252	31,753
	31	left	30,616.21	30,522	239.26	30,282	31,800
	29	right	30,223.57	30,107	288.08	29,690	31,439
	29	left	30,216.88	30,090	295.11	29,813	31,450
	25	right	29,816.64	29,639	324.37	29,381	30,575
	25	left	29,848.58	29,681	346.49	29,370	30,585
	24	right	30,139.59	30,039	289.3	29,690	31,486
	24	left	30,080.3	30,031	246.95	29,720	31,489
	19	right	30,140.02	30,060	269.77	29,563	31,504
	19	left	30,091.06	30,016	260.38	29,591	31,477

Figure 5 illustrates the distribution histogram of pixel intensity values from thermal images of diabetic patients' feet, grouped by their Semmes Weinstein test results (either positive/abnormal or negative/normal). For the patients with abnormal results (Patient-14 right, Patient-26 left, and Patient-27 left), the histograms show a broader range of pixel intensities with noticeable peaks, indicating variations in tissue temperature that could correspond to areas of concern such as inflammation or infection. The distributions are uneven, suggesting significant differences in temperature across the foot. Conversely, the histograms for patients with normal Semmes Weinstein results (Patient-19 left, Patient-29 right, and Patient-35 left) exhibit more concentrated pixel intensity distributions, with fewer and less pronounced peaks. This pattern suggests a more uniform thermal profile, indicative of healthy tissue without significant temperature variations. The differences in histogram shapes between the two groups underscore the potential of thermal imaging in differentiating between normal and abnormal conditions in diabetic feet.

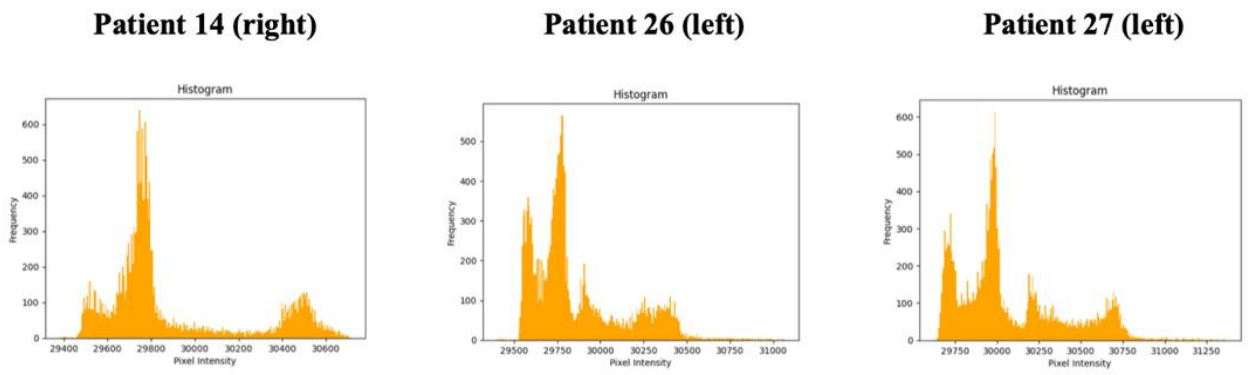

(a)

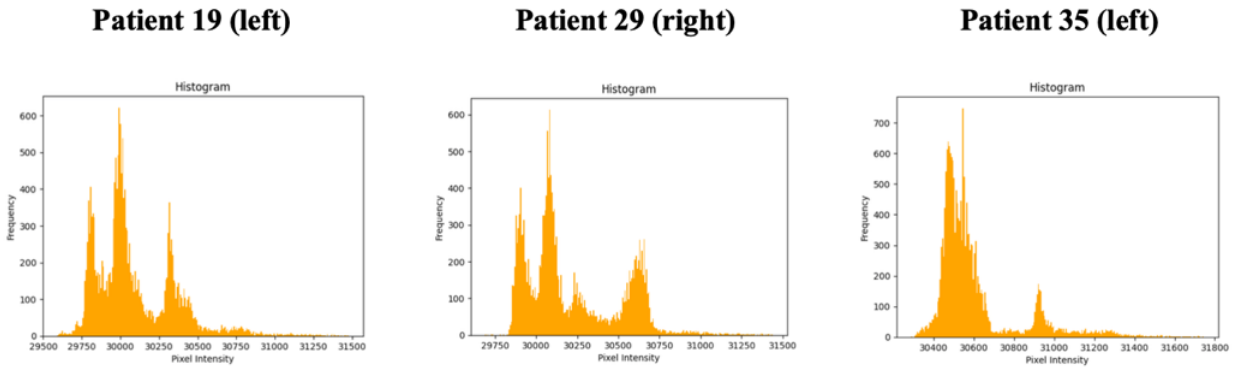

(b)

Figure 5. The PHOOTONICS image descriptors for the Semmes Weinstein for **(a)** (abnormal) and **(b)** for negative, normal case.

7.3. Diabetic foot classification based on the Colour Duplex Ultrasound (CDU)

Table 5 presents descriptive statistics of pixel intensity from thermal images for patients with diabetic foot ulcers, categorized based on the degree of stenosis as determined by ultrasound (U/S) imaging: clinically important stenosis, mild stenosis, and no stenosis. For patients with clinically important stenosis, the mean pixel intensity ranges from 30,042.97 to 30,688.82, with relatively high standard deviations, indicating significant variability in thermal patterns. This may suggest more extensive tissue damage or inflammation in areas of critical stenosis, as reflected by higher variability in thermal responses.

In comparison, patients with mild stenosis exhibit mean pixel intensities similar to those with clinically important stenosis, but the standard deviations are generally lower, indicating less variation in tissue temperature. This suggests that while there may be some temperature anomalies in these patients, the thermal patterns are more consistent than in those with more severe stenosis. For patients without stenosis, the pixel intensity values appear somewhat higher on average, with means ranging from 29,987.27 to 30,615.35. These patients generally show lower variability in thermal responses, as reflected by the smaller standard deviations, which could be indicative of more stable tissue temperatures and less inflammation or damage. The thermal imaging data thus provides valuable insight into the severity of foot conditions associated with varying levels of stenosis in diabetic patients.

Table 5. Statistical analysis for ultrasound stenosis.

U/S stenosis	Patient ID	Left/Right Foot	Thermal Values				
U/S clinically important stenosis			**Mean**	**Median**	**Sd**	**Min**	**Max**
	36	right	30,688.82	30,601	209.58	30,238	31,753
	36	left	30,703.60	30,618	206.7	30,417	31,764
	33	right	30,466.64	30,417	144.62	30,215	31,282
	33	left	30,434.64	30,371	157.64	30,199	31,192
	32	left	30,592.40	30,510	199.11	30,302	31,636
	31	right	30,586.31	30,481	250.86	30,252	31,753
	31	left	30,616.21	30,522	239.26	30,282	31,800
	30	right	30,420.97	30,367	193.83	30,070	31,605
	30	left	30,377.36	30,330	171.13	30,131	31,614
	27	right	30,093.33	29,985	331.02	29,462	31,404
	27	left	30,081.56	29,983	319.93	29,624	31,365
U/S mild stenosis							
	32	right	30,642.08	30,569	198.25	30,168	31,693
	31	right	30,586.31	30,481	250.86	30,252	31,753
	31	left	30,616.21	30,522	239.26	30,282	31,800
	14	right	29,896.95	29,769	323.74	29,381	30,712
	14	left	29,826.08	29,707	313.34	29,401	30,626
U/S no stenosis							
	35	right	30,621.73	30,544	206.58	30,211	31,744
	35	left	30,605.27	30,538	208.21	30,288	31,744
	28	right	29,987.27	29,943	175.49	29,690	30,941
	28	left	30,315.35	30,244	210.81	30,008	31,441

Figures 6–10 depict the histograms of the distribution of pixel intensity values from thermal images of diabetic foot patients, categorized by the severity of stenosis determined through ultrasound (U/S). For patients with clinically important stenosis (Patient-32 left, Patient-33 left, and Patient-36 right), the histograms show multiple peaks and broader intensity ranges, indicating a more heterogeneous temperature distribution likely due to significant vascular complications affecting foot tissue temperature. Patients with mild stenosis (Patient-14 right, Patient-31 left, and Patient-32 right) display histograms with slightly narrower distributions, reflecting more consistent pixel intensities but still some variation, which suggests moderate alterations in foot temperature patterns. In contrast, the histograms for patients without stenosis (Patient-28 left, Patient-35 left, and Patient-35 right) exhibit sharper, more concentrated peaks and tighter distributions, suggesting a more uniform temperature profile. This uniformity reflects healthier vascular conditions with less thermal variation, indicating fewer complications. Overall, the histograms reveal that the severity of stenosis correlates with increased variability in foot temperature, with more severe cases showing greater dispersion in pixel intensity.

Patient 32 (left) **Patient 33 (left)** **Patient 36 (right)**

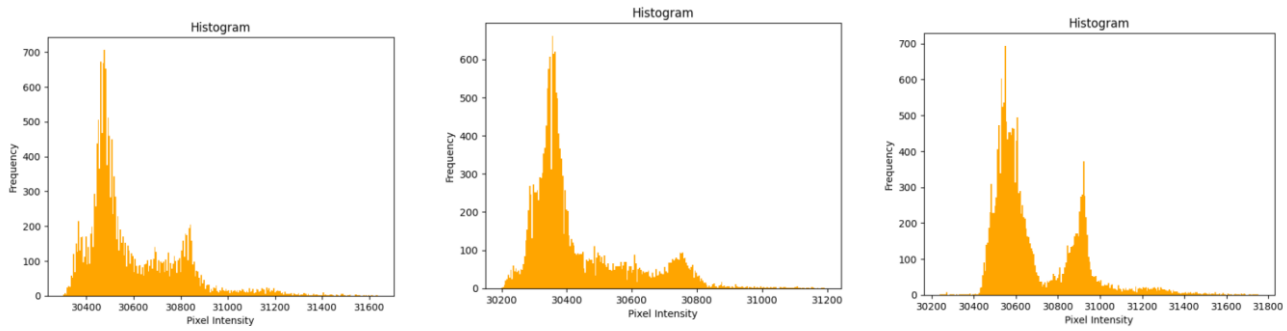

Figure 6. PHOOTONICS image features for the important stenosis subclass assessed by CDU.

Patient 14 (right) **Patient 31 (left)** **Patient 32 (right)**

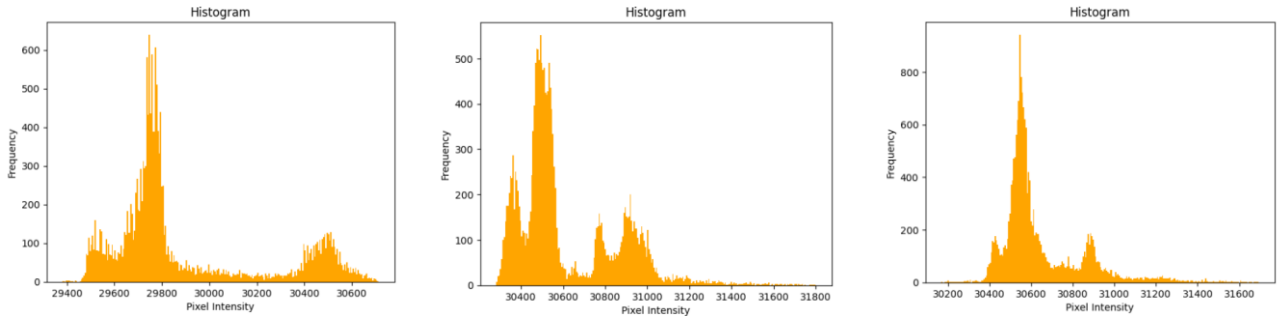

Figure 7. PHOOTONICS image features for the mild stenosis assessed by CDU.

Patient 28 (left) **Patient 35 (left)** **Patient 35 (right)**

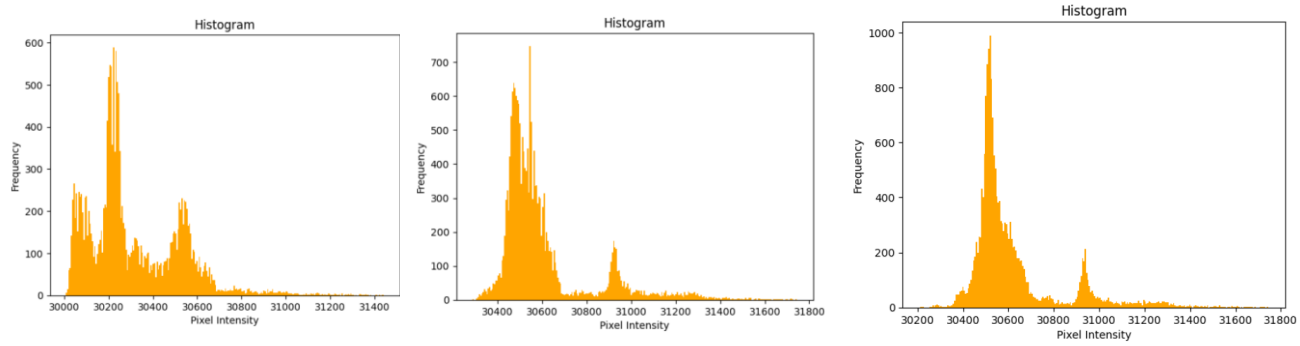

Figure 8. PHOOTONICS image features for the no stenosis assessed by CDU.

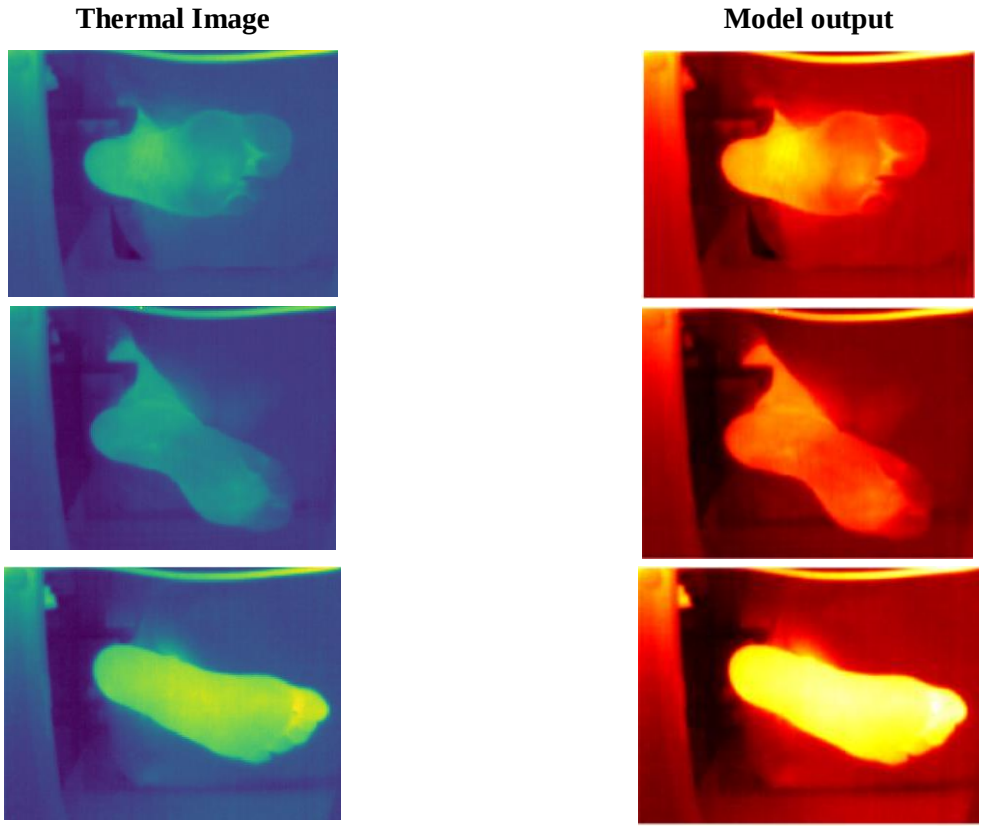

Figure 9. DF with active ulcer as it has been processed by the AI neural network model.

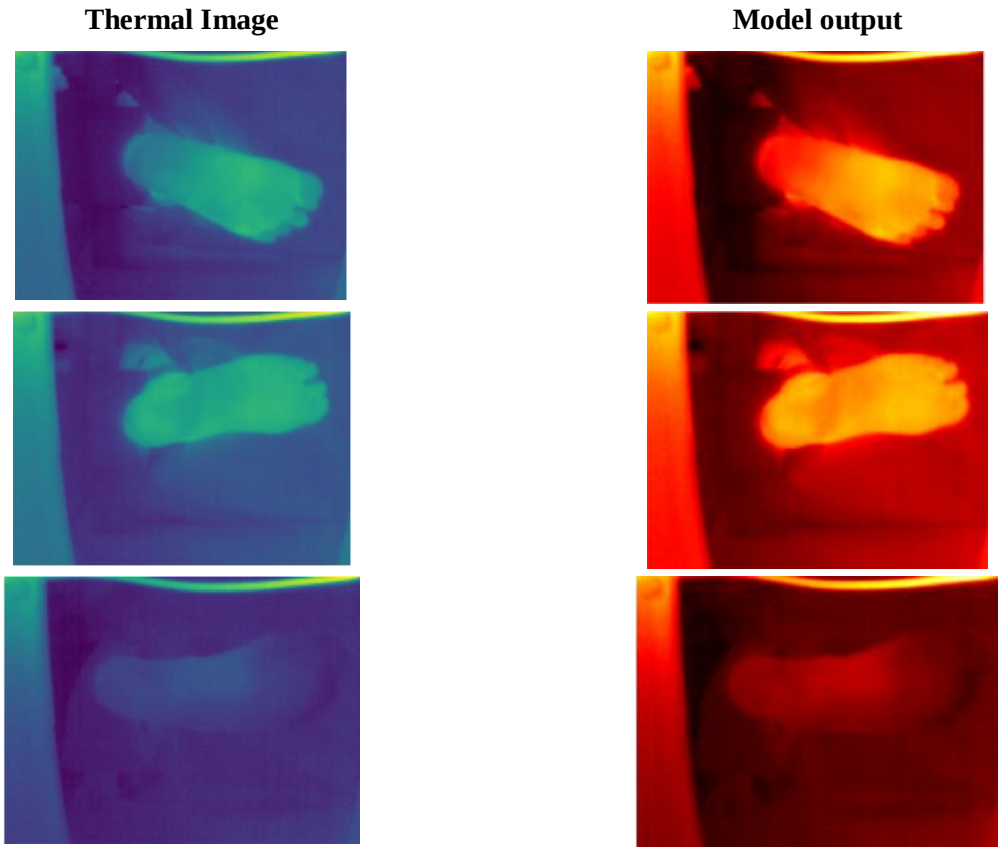

Figure 10. DF with recovered ulcer as featured has been extracted by the AI-model.

8. AI feature extraction model results

The ResNet18 model, a deep residual network architecture, was utilized for feature extraction in the analysis of DFUs. Leveraging its pre-trained capabilities on ImageNet, ResNet18 effectively extracted high-level features from DFU images, which were critical for distinguishing various ulcer conditions. The model's architecture, consisting of 18 layers with skip connections, allowed for a robust learning process, minimizing the vanishing gradient problem and ensuring that essential patterns and textures were captured. These features were then fed into subsequent classifiers, yielding promising results in differentiating between various stages and types of diabetic foot ulcers. The use of ResNet18 significantly enhanced the performance of the overall diagnostic pipeline, as evidenced by increased accuracy and reduced false-positive rates in the experimental evaluations.

The following figures depicts that the results of ResNet18's feature extraction were well-suited for the complexities associated with DFU images. The extracted features were highly discriminative, leading to improved classification outcomes in comparison to traditional feature extraction methods. Notably, the model showed a strong performance in detecting subtle textural differences in ulcers, which are often indicative of early or advanced stages of the condition. Overall, the integration of ResNet18 for feature extraction not only streamlined the analytical process but also provided a reliable foundation for developing automated diagnostic tools for diabetic foot ulcer management. Analysis of thermal and multispectral image data sets is performed using AI neural network structure.

Figures 9–13 display a set of thermal images and corresponding model outputs for DFUs with active ulcers. On the left side, three thermal images show the feet of diabetic patients, each visualized in a colour gradient that ranges from cooler tones (blue) to warmer tones (green and yellow), indicating different temperature levels. Areas with higher temperature, possibly due to inflammation associated with active ulcers, appear in lighter green or yellow, while cooler regions are depicted in blue.

On the right side, the corresponding model outputs are shown. These images are in a different color scale, primarily using a heat map that ranges from dark red to bright yellow. The model output images highlight regions with higher thermal intensity using bright yellow and red colors, which correspond to the areas suspected of having active ulcers. This visualization suggests that the model is capable of identifying and emphasizing regions of increased thermal activity that may indicate the presence of an active ulcer, thereby aiding in the detection and diagnosis of diabetic foot complications. The differences in color representation between the thermal images and model outputs underscore the model's ability to process and interpret thermal data for clinical insights effectively. The AI toolkits have been optimized in terms of parameter selection using a Bayesian optimization approach.

Apart from the PHOOTONICS HOME device, ATTIKON university hospital also caried out clinical trials for the PHOOTONICS PRO device. In particular, the PRO device was tested on 7 participants and created a hyperspectral, with more than 120 bands, and a thermal dataset. Some indicative results are presented in the following figures.

In Figure 12 the hyperspectral image was converted into RGB by selecting the 3 bands, out of the 120, that corresponds to the RGB format. Hyperspectral images with 120 bands provide significantly more detailed information compared to traditional RGB images when identifying ulcers on diabetic feet. Unlike RGB images, which only capture light in three broad bands (red, green, and blue), hyperspectral imaging captures light across 120 narrow spectral bands, spanning a wide range of wavelengths. This

allows for the detection of subtle differences in biochemical properties that are not visible in standard RGB images. As a result, hyperspectral imaging can more accurately differentiate between healthy and ulcerated tissue, detect early signs of ulcer formation, and assess the extent and severity of ulcers, leading to more precise diagnosis and improved treatment planning for diabetic patients. Figure 13 shows the results of the thermal image.

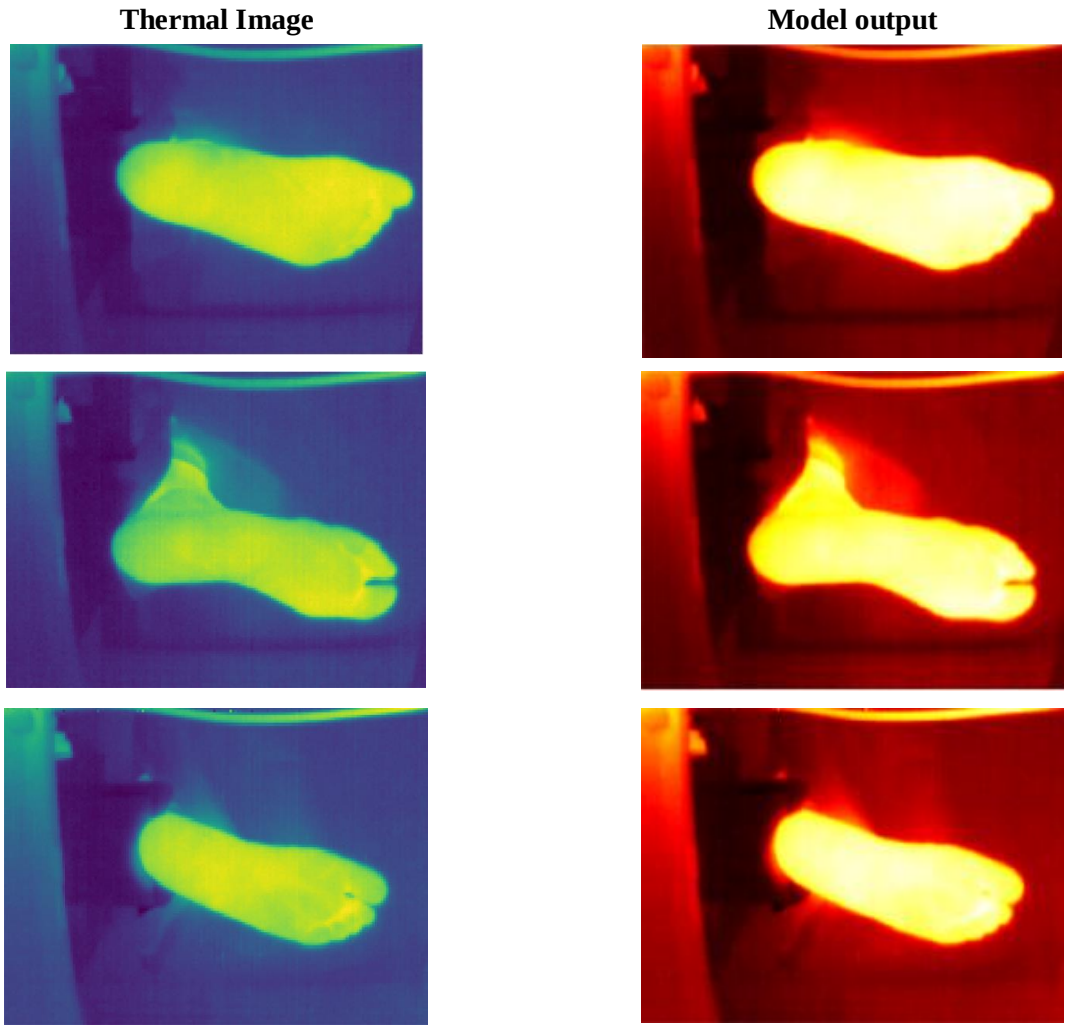

Figure 11. DF without ulcer as it has been processed by the AI neural network model.

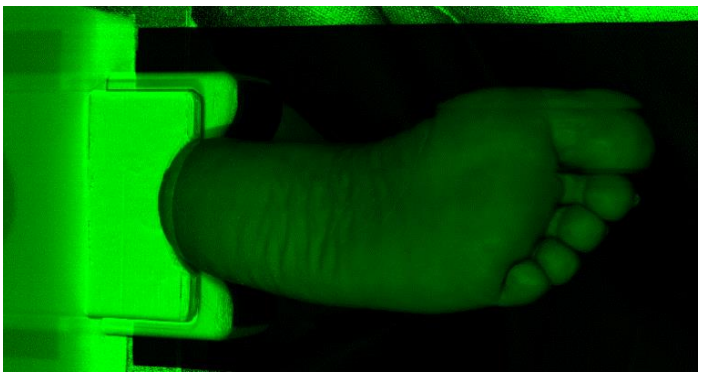

Figure 12. Hyperspectral image of the PRO device.

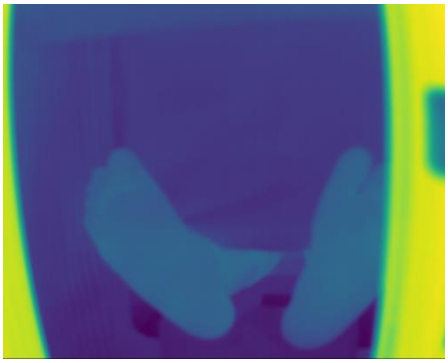

Figure 13. Thermal image of the PRO device.

Table 6 shows a comparative study of our approach with other methods such as region growing, the watershed segmentation algorithm, a feedforward neural network and our approach. For all models, four different modes of analysis are taken into account; the use of a single mode of either RGB, thermal or hyperspectral sensing and the cross-modal approach. The results show that our method yield better results than the compared ones. Among the single models the RGB images presents the lowest performance while hyperspectral and the thermal the best ones.

Table 6. A comparative study of our approach with other methods.

Compared Methods	Precision	Recall
Image Segmentation using region growing		
Only Thermal + Region Growing	75.4	71.1
Only RGB + Region Growing	63.2	59.8
Only Hyperspectral + Region Growing	74.2	78.5
Cross-Modality + Region Growing	78.3	76.2
Image Segmentation using Watershed		
Only Thermal + Watershed		
Only RGB + Watershed	76.2	73.2
Only Hyperspectral + Watershed	65.2	60.0
Cross-Modality + Watershed	78.9	77.5
Image Segmentation using Shallow Neural Networks		
Only thermal + Shallow Neural Networks	83.6	79.2
Only RGB + Shallow Neural Networks	78.5	74.7
Only Hyperspectral + Shallow Neural Networks	83.7	82.5
Cross-Modality ++ Shallow Neural Networks	87.4	86.9
Image Segmentation using the Proposed Deep Models		
Only Thermal + deep models	85.6	84.3
Only RGB + deep models	80.1	78.7
Only Hyperspectral + deep models	86.7	87.8
Cross-Modality + deep models—OUR APPROACH	90.4	89.6

9. Conclusions

This paper proposes the results of a clinical study executed across four European Hospitals to validate the effectiveness and efficiency of different types of photonics-based devices for early diagnosis and management of foot ulcers due to diabetes. The paper describes the recruitment procedure of the clinical study along with all the preparatory actions. It also proposes the clinical validation results in terms of achieving the main target objectives of the device. The common data template model used for annotating the data is also presented in this paper.

Finally, we have applied different AI-driven models for segmenting the foot ulcers and thus contributing towards an automated diagnosis and management procedure. The architecture adopted is based on ResNet model and the CNNs. The derived segmentation models shown results for ulcer prediction, wound delineation, diabetic foot ulcer classification into active ulcers, healed ulcers and feet without an active and/or healed ulcer. We have also presented traditional test for diabetic foot assessment like the Semmes Weinstein approach. In the latter case, we have a classification on positive (abnormal) and negative (normal) foot. Finally, we have conducted foot classification tests using color duplex ultrasound measuring stenosis and classifying it into important, mild and no stenosis respectively. The AI feature extraction model are the final results of the paper.

Data availability statement

The data have been generated during the H2020- PHOOTONICS project. The content of this paper can be shared to everybody (it is open) as well as the results and research achievements derived. The original data used for yielding the results are medical information of patients that should be protected due to privacy issues. We do not describe any original datum in any section of this paper.

Declaration of generative AI and AI-assisted technologies

The authors did not use generative AI or AI-assisted technologies in the writing of this manuscript.

Acknowledgments

This work has been funded by the project Photogrammetry and Geoinformatics of the National Technical University of Athens under grant agreement No. 95030400.

Authors' contribution

Conceptualization, methodology, formal analysis, investigation, resources, data curation, writing—original draft preparation, Ioannis Rallis, Aikaterini Angeli, Anastasios Doulamis and Nikolaos Doulamis; clinical study, Aikaterini Angeli; software, Ioannis Rallis; validation, Ioannis Rallis and Aikaterini Angeli; writing—review and editing, Nikolaos Doulamis and Anastasios Doulamis; visulation, Ioannis Rallis and Aikaterini Angeli; supervision, Nikolaos Doulamis; project administration, Ioannis Rallis and Aikaterini Angeli; funding acquisition, Nikolaos Doulamis and Anastasios Doulamis. All authors have read and agreed to the published version of the manuscript.

Conflicts of interest

Anastasios Doulamis holds the position of Editor-in-Chief for *Electronics and Signal Processing* and has not peer reviewed or made any editorial decisions for this paper.

References

[1] Acton QA. *Foot Diseases: Advances in Research and Treatment*. Atlanta: Scholarly Editions, 2011.
[2] World Health Organization. Diabetes Fact Sheet. 2016. Available: https://www.who.int/news-room/fact-sheets/detail/diabetes (accessed on 11 May 2026).

[3] Margolis DJ, Malay DS, Hoffstad OJ, Leonard CE, MaCurdy T, *et al.* Incidence of diabetic foot ulcer and lower extremity amputation among Medicare beneficiaries, 2006 to 2008. *Data Points Publication Series* 2011.

[4] Lu G, Fei B. Medical hyperspectral imaging: a review. *J. Biomed. Opt.* 2014, 19(1):010901.

[5] Mishchenko MI, Tuchin V. Tissue optics: light scattering methods and instruments for medical diagnostics, SPIE Press, Bellingham, WA (2007) Hardbound, ISBN 0-8194-6433-3, xl + 841pp. *J. Quant. Spectrosc. Radiat.* 2009, 110:528.

[6] Patterson MS, Wilson BC, Wyman DR. The propagation of optical radiation in tissue. II: optical properties of tissues and resulting fluence distributions. *Lasers Med. Sci.* 1991, 6(4):79–390.

[7] Joel M, Tuan VD. Chapter 2 Optical properties of tissue. In *Biomedical Photonics Handbook*. Boca Raton: CRC Press, 2003. pp. 1–76.

[8] Yang Q, Sun S, Jeffcoate WJ, Clark DJ, Musgove A, *et al.* Investigation of the performance of hyperspectral imaging by principal component analysis in the prediction of healing of diabetic foot ulcers. *J. Imaging* 2018, 4(12):144.

[9] Khaodhiar L, Dinh T, Schomacker KT, Panasyuk SV, Freeman JE, *et al.* The use of medical hyperspectral technology to evaluate microcirculatory changes in diabetic foot ulcers and to predict clinical outcomes. *Diabetes Care* 2007, 30(4):903–910.

[10] Doulamis A, Doulamis N, Angeli A. A cost-effective photonics-based device for early prediction, monitoring and management of diabetic foot ulcers. In *Proceedings of the 13th ACM International Conference on PErvasive Technologies Related to Assistive Environments*, Corfu, Greece, June 30–July 7, 2020, pp. 1–8.

[11] Doulamis A, Doulamis N, Angeli A, Lazaris A, Luthman S, *et al.* A non-invasive photonics-based device for monitoring of diabetic foot ulcers: architectural/sensorial components & technical specifications. *Inventions* 2021, 6(2):27.

[12] Li Z, Liu F, Yang W, Peng S, Zhou J. A survey of convolutional neural networks: analysis, applications, and prospects. *IEEE Trans. Neural Networks Learn. Syst.* 2021, 33(12):6999–7019.

[13] Du G, Cao X, Liang J, Chen X, Zhan Y. Medical image segmentation based on U-net: a review. *J. Imaging Sci. Technol.* 2020, 64(2):1–12.

[14] Takahashi S, Sakaguchi Y, Kouno N, Takasawa K, Ishizu K, *et al.* Comparison of vision transformers and convolutional neural networks in medical image analysis: a systematic review. *J. Med. Syst.* 2024, 48(1):84.

[15] Armstrong DG, Boulton AJM, Bus SA. Diabetic foot ulcers and their recurrence. *N. Engl. J. Med.* 2017, 376(24):2367–2375.

[16] Mishra B. Role of Ankle Brachial Index (ABI) in management of non-healing ulcers of lower limb. *J. Univers. Surg.* 2018, 6(1):7.

[17] Goyal M, Reeves ND, Davids K, Bowling FL. Addressing the gaps in diabetic foot ulcer research: a focus on deep learning. *Front. Bioeng. Biotechnol.* 2021, 9:647528.

[18] Mukherjee R, Chatterji S, Manohar DD, Das A, Pal A. A deep learning based model for automated diabetic foot ulcer detection and classification. *IEEE J. Transl. Eng. Health Med.* 2020, 9:1900314.

[19] Bharara M, Cobb JE, laremont DJ. Thermography and thermometry in the assessment of diabetic neuropathic foot: a review of the literature. *The Foot* 2006, 16(4):297–298.

[20] Sørensen BM, Johansen NB, Kawohl W, Ramlau-Hansen CH, Ängquist L, *et al.* Prospective association between short sleeping duration and diabetes in adults: the MONICA/KORA Augsburg cohort study. *Diabetes Care* 2016, 38(8):1462–1471.

[21] Orlin MN, McPoil TG. Plantar pressure assessment. *Phys. Ther.* 2000, 80(4):399–409.

[22] Tulloch J, Zamani R, Akrami M. Machine learning in the prevention, diagnosis and management of diabetic foot ulcers: a systematic review. *IEEE Access* 2020, 8:198977–199000.

[23] Yap MH, Ng CC, Chatwin K, Abbott CA, Bowling FL, *et al.* Computer vision algorithms in the detection of diabetic foot ulceration: a new paradigm for diabetic foot care? *J. Diabetes Sci. Technol.* 2016, 10(2):612–613.

[24] Tzortzis IN, Davradou A, Protopapadakis E, Kaselimi M, Doulamis N, *et al.* Unsupervised diabetic foot monitoring techniques. In *Proceedings of the 15th international conference on PErvasive technologies related to assistive environments*, New York, USA, June 29–July 1, 2022, pp. 608–614.

[25] Baseman C, Fayfman M, Schechter MC, Ostadabbas S, Santamarina G, *et al.* Intelligent care management for diabetic foot ulcers: a scoping review of computer vision and machine learning techniques and applications. *J. Diabetes Sci. Technol.* 2025, 19(3):820–829.

[26] Ramakrishnan J. Synergizing IoT and machine learning for diabetic foot ulcer detection and management. *Int. J. Syst. Assur. Eng. Manag.* 2025, 16(11):3614–3625.

[27] Fadhel MA, Alzubaidi L, Gu Y, Santamaría J, Duan, Y. Real-time diabetic foot ulcer classification based on deep learning & parallel hardware computational tools. *Multimedia Tools Appl.* 2024, 83(27):70369–70394.

[28] Kaselimi M, Protopapadakis E, Doulamis A, Doulamis N. A review of non-invasive sensors and artificial intelligence models for diabetic foot monitoring. *Front. Physiol.* 2022, 13:924546.